Spectral mixture analysis method based on the simulation of real scenario

FAN Weiliang, DU Huaqiang, ZHOU Guomo, XU Xiaojun, CUI Ruirui, DONG Dejin

Zhejiang Provincial Key Laboratory of Carbon Cycling in Forest Ecosystems and Carbon Sequestration, *Zhejiang Agriculture and Forestry University*, *Zhejiang Lin'an* 311300, *China*

Abstract: This paper proposes a new unmixing method based on the simulation of real scenario. Fractions of the components are firstly obtained through the real scenario simulation. Then reflectance values of the endmembers (simulated endmembers) are calculated by combining the image reflectance values and corresponding simulated fractions. A constrained linear model is finally used to unmix pixels based on the simulated endmembers. Comparative analysis of the different endmember extraction methods, such as simulated endmembers, image endmembers, and reference endmembers, indicates that the simulated endmember method has the highest estimation accuracy and robustness for the crown closure of moso bamboo. The advantage of the real scenario simulation is to use field data as a priori knowledge for endmember extraction and introduce a three-dimensional simulation model into a two-dimensional linear spectral decomposition.

Key words: real scenario modeling, simulated endmember, spectral mixture analysis, linear mixture models, Landsat TM

CLC number: TP751 **Document code:** A

Citation format: Fan W L, Du H Q, Zhou G M, Xu X J, Cui R R and Dong D J. 2010. Spectral mixture analysis method based on the simulation of real scenario. *Journal of Remote Sensing*. **14**(6): 1241—1258

1 INTRODUCTION

Remote sensing image, as a common information carrier, represents land cover attributes within pixel units. A variety of surface components or different states of surface component have significant impact on the information acquired by remote sensing images in pixel scale, which are known as *mixed pixels*. It not only influences the accuracy of land cover classification, but also strongly hinders the development of quantitative remote sensing (Yang *et al.*, 2008). Corresponding unmixing methods are proposed for mixed pixel issues (Ichoku & Karnieli, 1996; Roberts *et al.*, 1998). Zhao (2003) summarized different spectral mixture analysis methods including linear model, geometric optics model, random geometric model, probability model and fuzzy model.

Endmember quality is the most important factor that affects the results of spectral mixture analysis (Zhao, 2003). At present, there are two main methods for endmember extraction as following:

The first one is *image endmembers* method, which determines endmembers from remote sensing image through different analytical methods. This method is commonly used in many studies and does not require field spectral measurements and prior knowledge (Woodcock *et al.*, 1994, 1997; Scarth & Phinn, 2000; Franklin & Turner, 1992). However, one issue existing in unmixing process is that *pure pixels* in remote sensing image often can not be found (Tompkins *et al.*, 1997; Tao *et al.*, 2008). For example, Li (1985, 1986, 1992) proposed the famous geometrical optical model, which included *four components*, such as sunlit vegetation, shadowed vegetation, sunlit background and shadowed background. In practice, full pure pixels of the four components are not within remote sensing images. Clean and deep water is often used to replace shadowed components (Hall *et al.*, 1995) or relatively pure pixels are collected from two-dimensional scatter plot of the brightness and greenness components derived from Tasseled cap transformation (Li & Strahler, 1985; Woodcock *et al.*, 1994, 1997). Therefore, *image endmembers* method is difficult to represent real attributes of land cover.

The second one is *reference endmembers* method, which determines endmembers using field spectrum measurement or spectral library (Rashed *et al.*, 2003). Characteristics of ground objects can be more accurately represented by Reference endmembers in theory，but remote sensing images are affected by the atmosphere, terrain, sensors, and many other potential factors. It is also difficult to represent spectral characteristics of ground objects in remote sensing images. In addition, reference endmembers can only represent a certain category of ground

Received: 2009-10-15; **Accepted**: 2010-05-15

Foundation: National Natural Science Foundation Project (No. 30700638), '948' item of National Forestry Bureau (No. 2008-4-49), items of science and technology department of Zhejiang province (No. 2007C13041 and No. 2008C12068).

First author biography: FAN Weiliang (1984—), male, Master candidate. He majors in forest management. He has published 1 article. E-mail: fanweiliang@163.com

Corresponding Author: DU Huaqiang, E-mail: dhqrs@126.com

objects' reflectance. High error or mistake will result from some kinds of endmembers loss in application.

Three-dimensional modeling of vegetation has been widely used in agriculture, forestry, ecology, remote sensing and many other fields (Guo & Li, 2001). Disney (2000) summarized many generating scenarios methods applied in remote sensing. With rapid development of computer technology, graphics algorithms, and emerging of three-dimensional measurement and modeling of vegetation (Prusinkiewicz, 1998), universal models for variety of situations continue to be developed (Liang, 2009). Model accuracy will be improved by more accurate simulation of vegetation canopy, however, the biggest obstacle of the stand-scale scenario details simulation is so many facets in scenario that causes time-consuming for computer calculation (Lei *et al.*, 2006). A simplified model has been used in many studies, and produces good results (Morsdorf *et al.*, 2004; Li & Strahler, 1985, 1986).

The sensor acquires sunlight reflection from four components in real forest scenario as mentioned above. Due to the disadvantages of the *image endmembers* and *reference endmembers*, this study simulates the real scenario of moso bamboo forest based on the simplified vegetation model. Fractions of the four components are obtained from simulated scenarios, and the reflectance of four components is inverted based on least squares method (*simulated endmembers*, the same below). Finally, fractions of non-modeled pixels are estimated using the fully constrained least squares linear spectral analysis method with simulated endmembers. In order to evaluate the three methods, such as image endmember method, reference endmember method and simulated endmember method, a comparative analysis of the different unmixing results is proposed. This study provides a new way of thinking, a new method for spectral mixture analysis, and a new technology for accurate retrieval of vegetation biophysical parameters from remote sensing data.

2 RESEARCH METHODS

2.1 Plot data collection and remote sensing image preprocessing

Anji County, located in Zhejiang Province, China, was selected as the study area, and the field work has been conducted during 19 August and 3 September 2008. A total of 55 moso bamboo sample plots with the size of 30 m×30 m per plot were allocated. The survey items in each plot included diameter at breast height (DBH), stem density and the coordinate of plots. The clown closure was measured by forestry experts in Zhejiang Agricultural and Forestry University and professionals in Anji country forestry bureau based on visual method described in the "Forest resources investigation and technical regulations" issued by State Forestry Administration in 2003. The relative errors of crown closure are less than 10%. The spectral reflectance of four components of moso bamboo forest was determined by the average values of several measurements using the ASD spectrometer on September 6, 2009. Because of the same season between spec- tral measurement and field investigation, the hyper spectral reflectance can well represent the characteristics of four components of moso bamboo forest.

The height and stock height were calculated using the model established by Zhou (1981), and the crown diameter was calculated according to references (Zhou, 1982). The correla- tion coefficient between estimated and measured (September 30, 2008) crown diameter is 0.88. These attributes were used as parameters of scenario simulation.

Landsat Thematic Mapper (TM) image acquired on July 5, 2008, was used in this study. This TM image was rectified by using control points taken from 1:50000 topographic maps, with the root mean square errors (RMSE) of 0.29 pixels. The Fast Line of sight Atmospheric Analysis of Spectral Hypercubes (FLAASH) module in ENVI 4.4 software was used to conduct radiometric and atmospheric calibration for this TM image.

2.2 Linear mixture model

Linear mixture model supposed that the spectral response of mixed pixel is assumed to be the linear combination of the constitutional pure ground objects' signature and their ratios respectively. The spectral signature of a mixed pixel can be represented by the linear regression model as follows.

$$f_i = \sum_{j=1}^{n}(a_{ij}x_j) + e_i \tag{1}$$

where a_{ij} is the reflectance of component j(j=1, 2,⋯, n) in band i; x_j is the area ratio of component j in the pixel; e_i represents Gaussian noise of band i. In order to make the linear mixture model more precise and scientific to describe mixed pixels, the Sum-to-one constraint and the Non-negative constraint must be imposed on the linear mixture model, which are expressed as follows.

$$\sum_{j=1}^{n} x_j = 1 \tag{2}$$

$$x_j \geqslant 0 \tag{3}$$

2.3 Image endmembers

The pure spectral pixels are found in TM image using the Pixel Purity Index (PPI) method (Boardman *et al.*, 1995). Then, combined the original remote sensing image, the endmembers are collected from the N-dimensional scatter plot based on PPI. The optimal endmember of each component is determined after repeated experiments shown in Fig. 6 (a).

2.4 Reference endmembers

The hyper spectral reflectance of four components of moso bamboo forest is measured using the portable ASD instrument, such as sunlit canopy, shadowed canopy, sunlit background and shadowed background. The measured spectral reflectance

(Fig.1) is re-sampled and matched with the TM bands (TM1—5, TM7) based on the TM spectral response function as shown in Fig.6 (b).

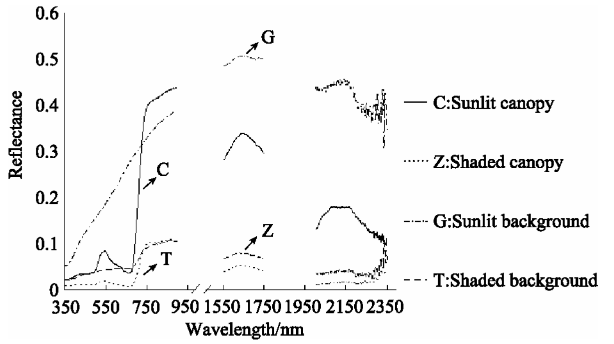

Fig. 1 Measured hyper spectral reflectance

In order to make the reference endmembers effective in pixel scale (Li *et al*., 1999), this study proposes the following assumptions according to the previous studies (Li *et al*., 1999; Raffy, 1994): there is no topography in pixel scale and the vegetation distribution patterns in pixel as same as the sub-pixel.

2.5 Scenario simulation and simulated endmembers

Firstly, 9 plots are randomly selected from 55 plots as the scenario simulation samples. The virtual three-dimensional scenario models are created using ground data (including plot orientation and slope information) and crown parameters of moso bamboo based on 3DMax9 software. In order to reduce the pieces in scenario models in pixel scale, the geometry of moso bamboo is simplified and the background of plot will be supposed as plane in this study. Then, according to certain solar height and azimuth information obtained from header file of remote sensing image, the shadow of ground objects is created using simulated sunlight in scenario. Four components fractions of simulated plot are calculated with top view (the same as TM sensor). Finally, combined the corresponding pixel reflectance and fractions of four components as shown in Eq.(4), the endmember reflectance of each band is estimated using least square method.

$$\boldsymbol{A}_i = (\boldsymbol{X}^{\mathrm{T}} \cdot \boldsymbol{X})^{-1} \cdot \boldsymbol{X}^{\mathrm{T}} \cdot \boldsymbol{F}_i \tag{4}$$

where $\boldsymbol{A}_i$ is the endmember reflectance vector of band i, $\boldsymbol{F}_i$ is the reflectance vector of band i for n pixels, $\boldsymbol{X}$ is the fractions of n pixels. Because this study sets plot group as 4, so Eq. (4) has well-posed or over-determined least squares solution when $n \geqslant 4$.

Each moso bamboo in 9 scenario samples is simplified as a simple geometry described as "stick" and "capsule" (Fig.2) according to the crown diameter, stick height, and height derived from DBH. Because there are too many culms per unit area (usually 150—500 culms/900m^2) and it is difficult to measure the location of each moso bamboo in dense forest, the coordinate of each moso bamboo in plot is not measured in this study. To solve this problem, each moso bamboo model is randomly located in scenario. The scenario model described above is established as shown in Fig.3. Each moso bamboo model is randomly located 10 times for No.2 sample. The results indicate the fractions range from 2% to 7% (Fig.4). Therefore, location of moso bamboo in plot has insignificant

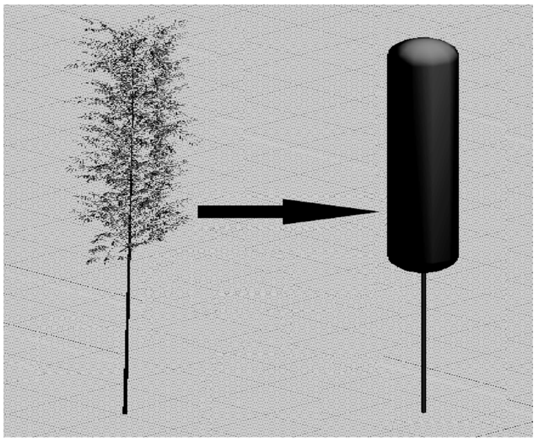

Fig. 2 Simplified bamboo model

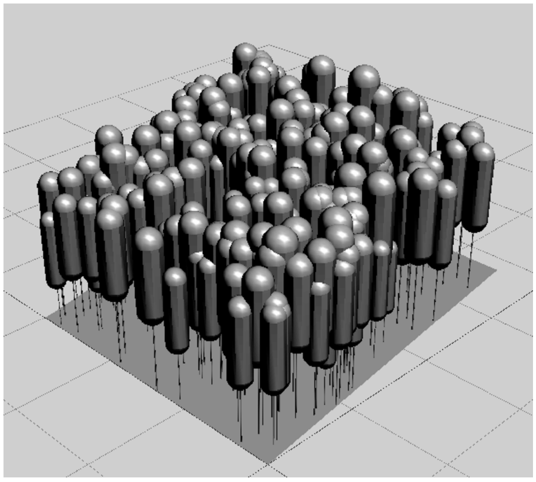

Fig. 3 Scenario component model

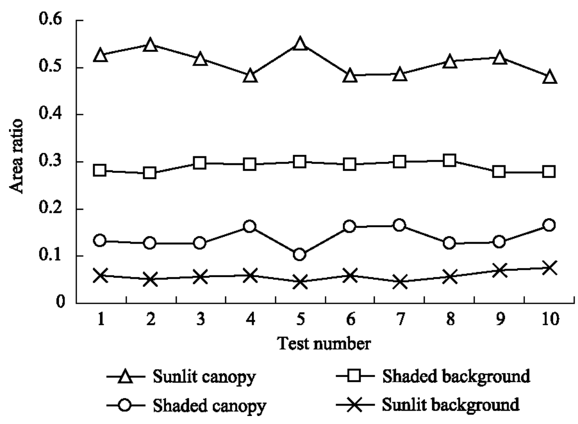

Fig. 4 Randomly location assignment experiments of bamboos on No.2 plot

effect on the fractions of four components. Any experiment for No.2 sample can be used to test scenario simulation method.

Fig.5 is the top view image of No.2 sample at the 5^{th} experiment, and it is easy to distinguish sunlit canopy, sunlit background and shadowed components from Fig.5(a). Fig.5(b) is the top view scenario model with no light source, and vegetation and non-vegetation can be easily distinguished. The four component fractions of sampling plots can be calculated based on the classification results of Fig.5(a) and Fig.5(b).

Due to clear edge problem of the simulated scenario, the illumination side of the sample plot has too much light back- ground and many of the crowns are beyond the plot boundary (Fig.5). In order to eliminate edge effects, the edge must be corrected to improve simulation results. This problem has been discussed (Li & Strahler, 1985). According to linear spectral mixture theory and the central 50% square area of image is unaffected by edge, this study only calculated the four components fractions using central 50% square area of top view image (Fig.5).

Total 9 randomly selected sample plots are established using scenario model, and fractions are determined through scenario simulation. The endmember reflectance is calculated using Eq.(4) (Fig.6 (c)).

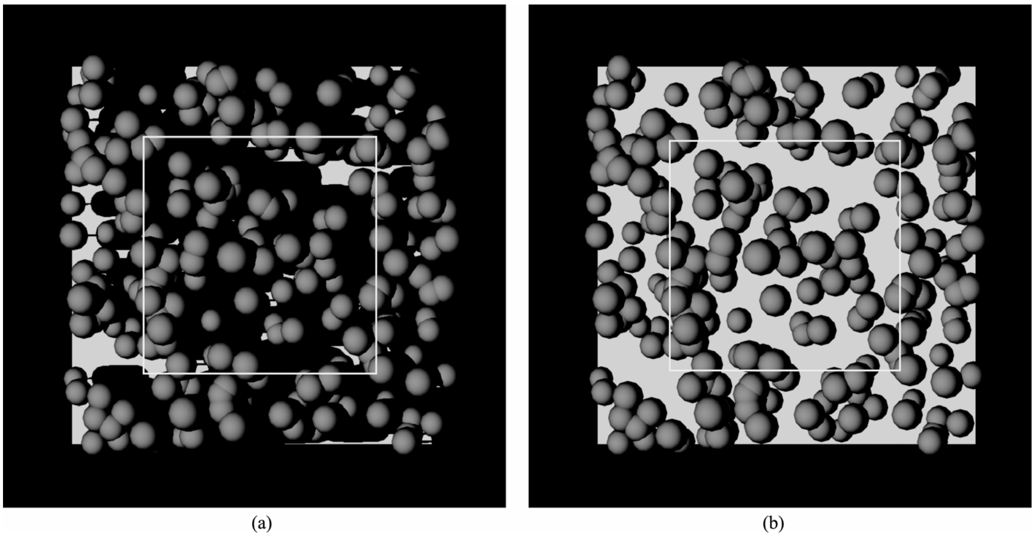

Fig. 5 Top view image of simulated scenario in 5^{th} test of No.2 sample
(a) Top view scenario model with light source; (b) Top view scenario model with no light source

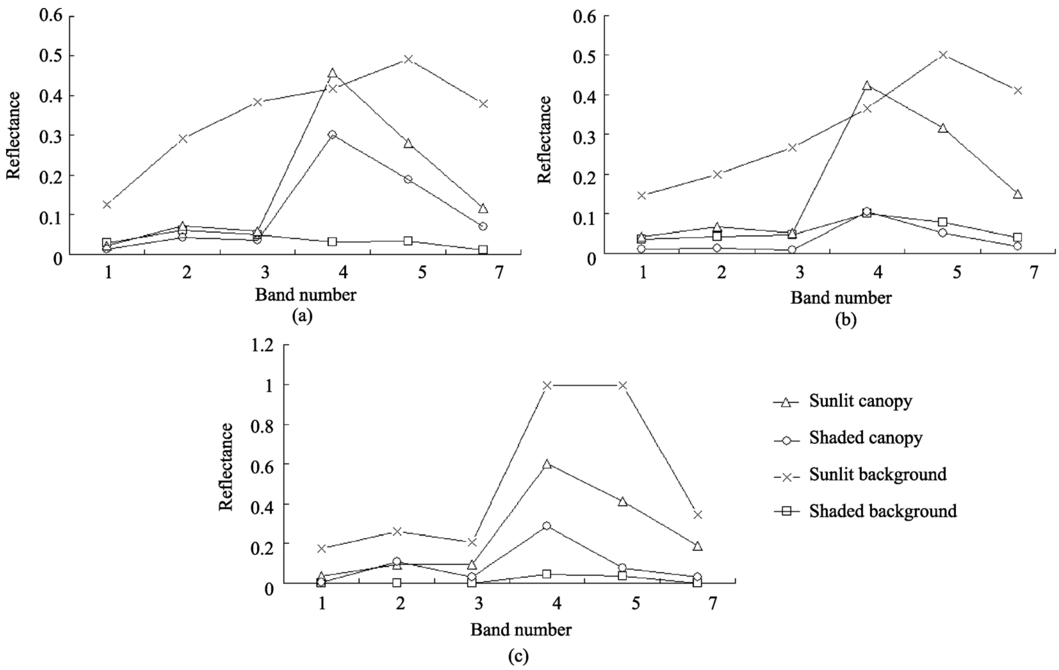

Fig. 6 Endmembers of the three methods
(a) Image endmembers; (b) Reference endmembers; (c) Simulated endmembers

2.6 Accuracy assessment method

Crown closure equals to the sum of sunlit canopy fraction and shadowed canopy fraction in top view image (Woodcock *et al.*, 1997). In this study, the spectral decomposition accuracy is assessed by comparing the measured crown closure with the estimation results using three types of endmembers.

3 RESULTS AND ANALYSES

3.1 Relationship between simulated and measured crown closure

There is a good linear relationship between simulated values and measured values for 9 samples' crown closure (Fig.7). In the case of medium crown closure (0.5—0.8), the simulation results are quite good; in the case of crown closure greater than 0.8, the simulated crown closure are slightly lower than the measured values. With the increase of crown closure, the crowns will overlap or fully overlap because of the randomly setting of coordinates (Chen & Leblanc, 1997).

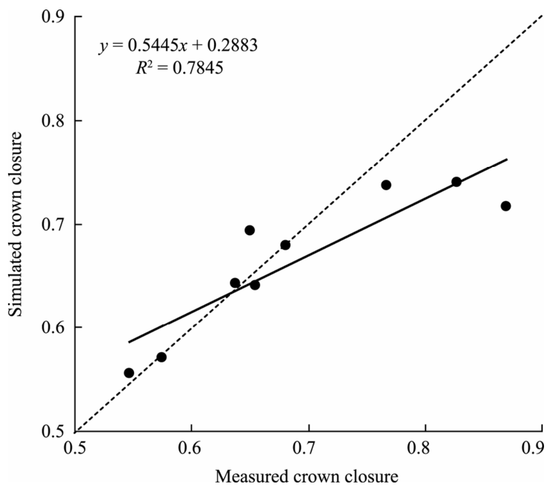

Fig. 7 Relationship between measured crown closure and simulated crown closure

3.2 The reflectance of the three types of endmember

The slightly differences between reference endmembers and image endmembers indicate that the field spectrum data without scaling can be better expression in the pixel scale (Fig.6). Reference endmembers of shaded canopy has a low reflectance in all bands because much sunlight is covered by shadow in the field measurement which causes the reference endmembers sharply decrease, especially for TM4.

The simulated endmembers has noticeable difference with other two. The sunlit canopy reflectance of simulated endmembers theoretically represents the canopy under sunlight with 100% crown closure. With the increase of leaves, TM reflectance of each band increases (Xu *et al.*, 2005), so the reflectance of simulated sunlit canopy very high. There are the same spectral characteristics of shadowed canopy between simulated endmembers and image endmembers, and both of them better represent the characteristics of vegetation. It is different between the sunlit background of image endmembers and reference endmembers which represent soil characteristics. The shadowed background of simulated endmembers shows vegetation characteristics. Meanwhile, because the shadowed background includes understory vegetation, litter, and many other factors, the shadowed background of simulated endmembers shows vegetation characteristics.

3.3 Accuracy assessment of spectral decomposition

The spectral decomposition results are assessed using the measured crown closure of 55 plots. The linear relationship between measured value and predicted values from image endmembers and reference endmembers are poor (Fig. 8). Majority of crown closure is overestimated with the relative error over 40% (Fig.9). A comparison analysis of the three types of endmember indicates that the image endmember method and reference endmember method overestimated the crown closure as they underestimate the endmember of sunlit canopy. The linear relationship between measured and predicted values using simulated endmembers is better than those using the other two endmembers (Fig.8(c)). The estimated error of crown closure (<10%) is acceptable (Liu & Wu, 2005), and Fig. 9 indicates only few plots' error beyond this range.

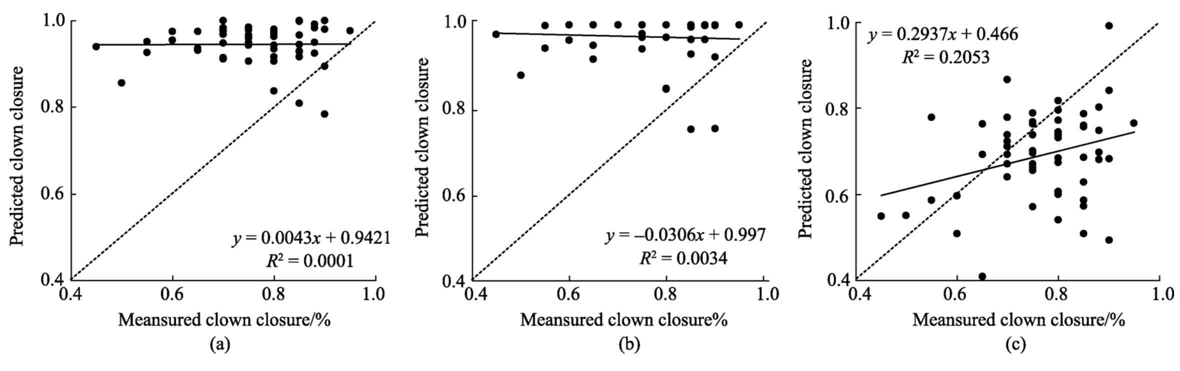

Fig. 8 Relationship between measured and simulated of crown closure for the 55 plots
(a) Image endmembers; (b) Reference endmembers; (c) Simulated endmembers

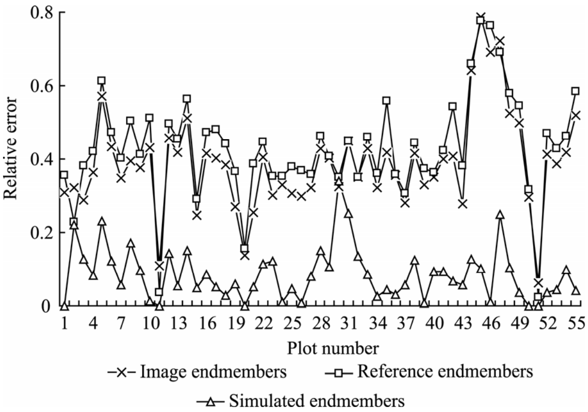

Fig. 9 Relative error between simulated and measured crown closure for the 55 plots

3.4 Experiment

In order to further compare the effect of three different methods, a large moso bamboo forest area selected from TM images (196 rows, 172 columns) was tested. This study area contains a small amount of roads and towns and does not include any scenario modeling samples.

Fig. 10 is the spectral decomposition results of the study area using these three unmixing methods. Because the two background fractions in moso bamboo area are close to 0 and the difference between the two canopy fractions in shady slope and sunny slope are exaggerated, the estimations from image endmember method are obviously discrepant with observations. Sunlit canopy fraction of reference endmembers is close to 100% while the other three fractions are close to 0. The fraction of sunlit canopy is overestimated, and the other three fractions are underestimated. Compared with the other two methods, the fractions from simulated endmember method are reasonable and uniformly distributed in image, which is consistent with the characteristics of moso bamboo forest (Zhang *et al.*, 2007).

The crown closure distribution and its histograms from different methods are shown in Fig.11, which further explain the results from numerical aspects. Compared with the measured crown closure, the estimation of image endmember method are overestimated. The distribution of estimations from reference endmember method has a huge different with measured values. The results of simulated endmember method are similar to the measured values, which further explaines that it is superior to the other two methods.

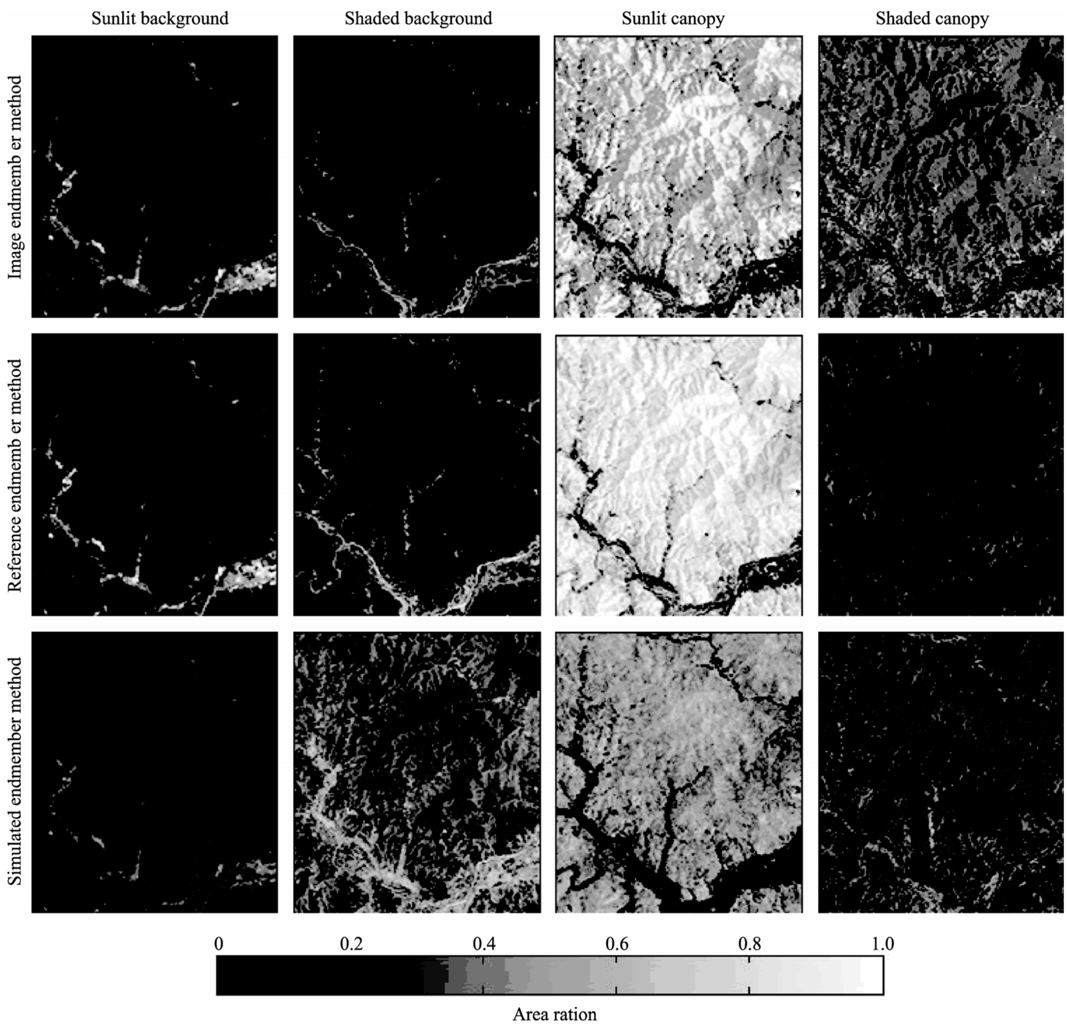

Fig. 10 Image decomposition result based on the three endmember

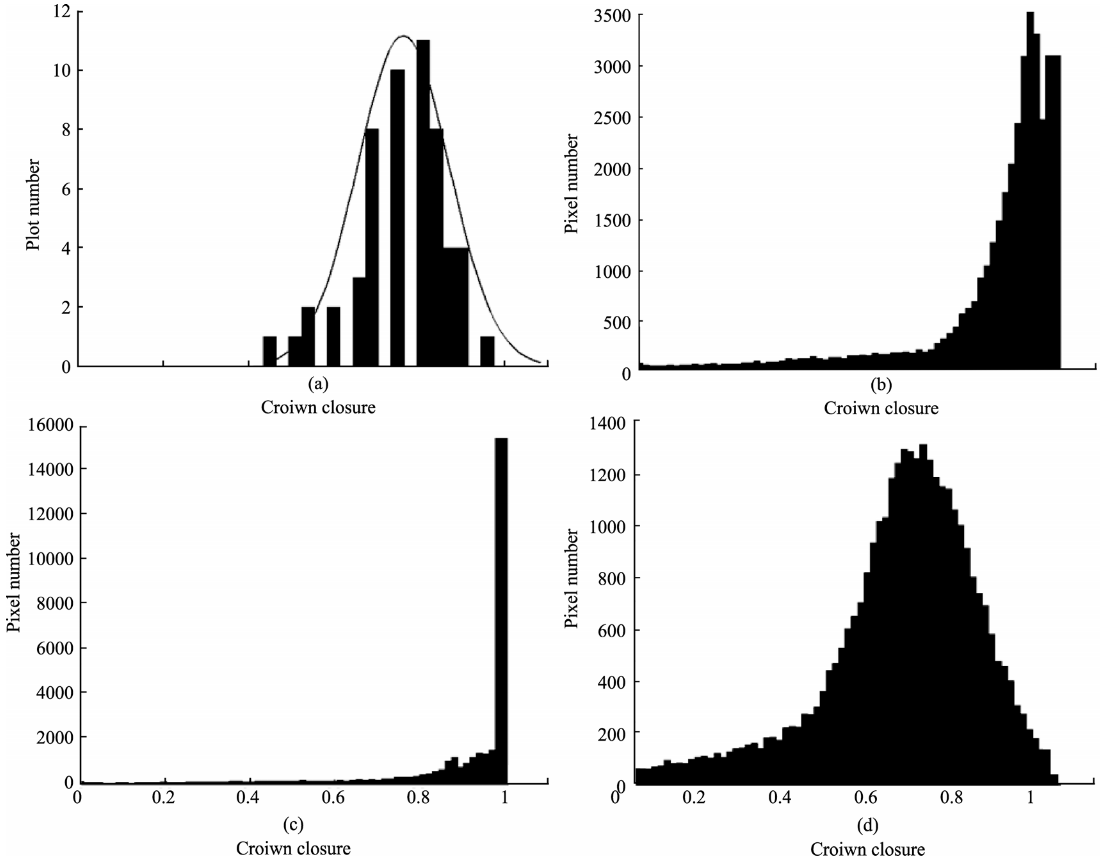

Fig. 11 Clown closure distribution of test image based on the 55 plots and the three spectral decomposition methods
(a) Meansured values; (b) Image endmember method; (c) Reference endmember method; (d) Simulated endmember method

4 DISCUSSION

4.1 Scenario simulation and accuracy assessment

Fractal method and computer graphics method were widely used in vegetation three-dimensional modeling and achieved very good results (Garcia & Sommer, 2006; Disney, *et al.*, 2006). However, how to optimize the number of pieces in stand-scale scenario is an urgent problem. Taken this study as an example, the scenario model can be simplified according to the real needs and research target in practical applications. It not only saves a lot of time and space, but also helps to discover the mechanism and nature of the problem. Therefore, the scenario simulation introduces the simplified vegetation model and achieves good results.

In this study, although the scenario simulation achieved good results, there is still some issues worthing of being explored. Firstly, there needs a lot of ground field data and crown parameters as prior knowledge for scenario modeling, and how to extract useful information from the prior knowledge as a basis of the simplification should be investigated. Secondly, the error sources in the process of scenario simulation should be analyzed. The accuracy of simulated endmember method is the highest compared with the other two methods (Fig.7), but the correlation coefficient is small (R^2=0.205). The estimated errors of some sample plots from the three methods are very high. The reason why those samples in high error should be analyzed before those excluded to improve accuracy. In addition, the background of plot is supposed to be flat in this study, because it is difficult to simulate the ups and downs in plot and its shadow. Although terrain of plot (30m×30m) slightly changes, it may still be part of the error sources of simulated endmembers. Finally, more attention should be paid to the quantity of sample plots of scenario modeling in future research. Only 9 samples randomly selected from 55 plots are used in this study, and how many samples can achieve the best result need further investigation.

Spectral mixture analysis method based on the simulation of real scenario is successfully applied in this study, and this method can also be applied in other types of ground objects.

4.2 Reflectance of endmembers and the linear spectral mixture analysis

Image endmembers is difficult to represent the real properties of ground objects as mentioned earlier. Although the result of the reference endmembers used in pixel scale after assumption is similar with the image endmembers, this will still cause some uncertainty (Li & Cai, 2005) and need further study. The simulated endmembers has good result. Firstly, the simulated endmembers can effectively represent the forest background information within pixel reflectance when the forest background is not selected as an endmember. Because the advantage of the simulated endmembers overcomes the dif- ficulty of the understory information extraction and the inco- mpleteness of endmembers selection, the simulated endmember method is more stable. Secondly, the reflectance of sunlit canopy in simulated endmembers is higher than other two endmembers (Fig.6). This implies that simulated endmembers are affected by other factors to some extent and obtained more "pure" sunlit canopy endmember. The simulated endmembers also overcomes the "impure" image endmembers. The back- ground of simulated endmembers can represent the understory information well in pixel scale, and the results of spectral mixture analysis are good.

The spectral mixture analysis includes 5 major models as mentioned above. Linear spectral mixture analysis is used in this study, and the performances of other methods need to be further analyzed.

There are several reasons for the entire TM image in Anji country was not used as experimental data. Firstly, the complex types of ground objects in research area will not help to visual interpretation when the entire image is used. Secondly, the full constraint least squares method used in this study requires abundance of product and inverse of matrix, which consume a large time (Tong, 2006). Third, the robustness of the real scenario modeling can be tasted when the experimental image does not contain the observed sample plots. Therefore, the simulated endmembers used in a large area still remain some technical issues, especially the complex of ground objects and mathematical algorithms.

5 CONCLUSIONS

The spectral mixture analysis methods are summarized in this study, and some problems are proposed. In order to overcome the limitation of the original spectral mixture me- thods, a scenario simulated method is introduced and used in moso bamboo forest. Then the simulated endmember method is compared with image endmember method and reference endmember method. The results indicates that the simulated endmember method has the highest precision and good robust performance. Subsequently, the performance of simulated endmember method is the best in application. The advantage of the real scenario simulation is to use field data as a priori knowledge for endmember extraction and introduces a three-dimensional simulation model into a two-dimensional linear spectral decomposition.

REFERENCES

Boardman J W, Kruse F A and Green R O. 1995. Mapping target signatures via partial unmixing of AVIRIS data: in Summaries. Fifth JPL Airbone Earth Science Workshop. JPL Publication 95—1, **1**: 23—26

Chen J M and Leblanc S G. 1997. A four-scale bi-directional reflectance model based on canopy architecture.*IEEE Transactions on Geoscience and Remote Sensing*, **35**: 1316—1337

Disney M I and Lewis S P. 2006. 3D modeling of forest canopy structure for remote sensing simulations in the optical and microwave domains. *Remote Sensing of Environment*, **100**: 114—132

Disney M I, Lewis S P and North P R J. 2000. Monte carlo ray tracing in optical canopy reflectance modeling. *Remote Sensing Reviews*, **18**(2—4): 163—196

Franklin J and Turner D L. 1992. The application of a geometric optical canopy reflectance model to semiarid shrub vegetation. *IEEE Transactions on Geoscience and Remote Sensing*, **30**(2): 293—301

Garcia-Haro F J and Sommer S. 2002. A fast canopy reflectance model to simulate realistic remote sensing scenarios. *Remote Sensing of Environment*, **81**: 205—227

Guo Y and Li B G. 2001. Research of review virtual plant.*Chinese Science Bulletin*, **46**(4): 273—280

Hall F G, Shimabukuro Y E and Huemmrich K F. 1995. Remote sensing of forest biophysical structure using mixture decomposition and geometric reflectance models. *Ecology Applications*, **5**(4): 993—1013

Ichoku C and Karnieli A. 1996. A review of mixture modeling techniques for sub-pixel land cover estimation. *Remote Sensing Reviews*, **13**: 161—186

Lei X D, Chang M, Lu Y C and Zhao T Z. 2006. A review on growth modeling and visualization for virtual trees. *Scientia Silvae Sinicae*, **42**(11): 123—131

Li S C and Cai Y L. 2005. Some scaling issues of geography. *Geographical research*, **24**(1): 11—18

Li X W and Strahler A H. 1985. Geometric-optical modeling of a conifer forest canopy. *IEEE Transactions on Geoscience and Remote Sensing*, **23**: 705—721

Li X W and Strahler A H. 1986. Geometrical-optical reflectance modeling of a conifer forest canopy. *IEEE Transactions on Geoscience and Remote Sensing*, **24**: 906—919

Li X W and Strahler A H. 1992. Geometric-optical bidirectional reflectance modeling of the discrete crown vegetation canopy: Effect of crown shape and mutual shadowing. *IEEE Transactions on Geoscience and Remote Sensing*, **30**: 276—291

Li X W, Wang J D and Strahler A H. 1999. Scale effects of planck law over a non-isothermal blackbody surface. *Science in China (Series E)*, **29**(5): 422—426

Liang S L. 2009. Quantitative Remote Sensing. (Fan W J Trans). Beijing: Science Press

Liu W and Wu E Y. 2005. Comparison of non-linear mixture models: sub-pixel classification. *Remote Sensing of Environment*, **94**: 145—154

Morsdorf F, Meier E, Kötz B, Itten K I, Dobbertin M and Allgöwer B. 2004. LIDAR-based geometric reconstruction of boreal type forest stands at single tree level for forest and wildland fire management. *Remote Sensing of Environment*, **92**(3): 353—362

Przemyslaw Prusinkiewicz. 1998. Modeling of spatial structure and development of plants: a review. *Scientia Horticulture*, **74**(1—2): 113—149

Raffy M. 1994. Heterogeneity and change of scale in models of remote sensing, Spatialization of multi-spectral models. *International journal of remote sensing*, **15**(12): 2359—2380

Rashed T, Weeks J R, Roberts D, Rogan J and Powell R. 2003. Measuring the physical composition of urban morphology using multiple endmember spectral mixture models. *Photogrammetric Engineering & Remote Sensing*, **69** (9): 1011—1020

Roberts D A, Batista G T, Pereira J L G, Waller E K and Nelson B W. 1998. Change identification using multi-temporal spectral mixture analysis. Applications in Eastern Amazonia. Remote Sensing Change Detection: Environmental Monitoring Applications and Methods. Michigan: Ann Arbor Press

Scarth P and Phinn S. 2000. Determining forest structural attributes using an inverted geometric-optical model in mixed Eucalypt forest, Southeast Queensland, Australia. *Remote Sensing of Environment*, **71**: 141—157

Tao X T, Wang B and Zhang L M. 2008. New scheme for decomposition of mixed pixels of remote sensing images based on nonnegative matrix factorization. *Information and Electronic Engineering*, **6**(1): 34—39

Tompkins S, Mustard J F, Pieters C M and Forsyth D W. 1997. Optimization of endmembers for spectral mixture analysis.*Remote Sensing of Environment*, **59**: 472—489

Tong Q X, Zhang B and Zheng L F. 2006. Hyperspectral Remote Sensing-Principles, Technology and Application. Beijing: Science Press

Woodcock C E, Collins J B, Gopal S, Jakabhazy V D, Li X W, Macomber S A, Ryherd S, Harward V J, Levitan J, Wu Y C and Warbington R. 1994. Mapping forest vegetation using Landsat TM imagery and a canopy reflectance model. *Remote Sensing of Environment*, **50**: 240—254

Woodcock C E, Collins J B, Jakabhazy V D, Li X W, Macomber S A and Wu Y C. 1997. Inversion of the Li-Strahler canopy reflectance model for mapping forest structure. *IEEE Transactions on Geoscience and Remote Sensing*, **35**(2): 405—414

Xu X R. 2005. Remote Sensing Physics.Beijing: Science Press

Yang W, Chen J, Song X W J, Gong P and Chen C X.2008.A new spectral mixture analysis method based on spectral correlation matching. *Journal of Remote Sensing*, **12**(3): 454—461

Zhang G H, Nie J Z and Xiao J H. 2007. Geostatistics analysis on the spatial pattern of Moso Bamboo.*Chinese Agricultural Science Bulletin*, **23**(12): 136—141

Zhao Y S. 2003. Principles and Methods of Analysis of Remote Sensing Applications. Beijing: Science Press

Zhou F C. 1981. Studys on the structure of culm form of phyllostachys pubescens. *Journal of Nanjing Technological College of Forest Products*, **1**: 16—69

Zhou F C. 1982. Studys on the structure of bamboo crown of phyllostachys pubescens. *Journal of Nanjing Technological College of Forest Products*, **3**: 46—73

模拟真实场景的混合像元分解

范渭亮, 杜华强, 周国模, 徐小军, 崔瑞蕊, 董德进

浙江农林大学 浙江省森林生态系统碳循环与固碳减排重点实验室, 环境科技学院, 浙江 临安 311300

摘　要: 在总结混合像元分解方法的基础上, 提出了一种模拟真实场景的像元分解方法, 该方法首先通过真实场景的模拟获得各分量的丰度, 结合遥感影像与场景模拟的丰度反演端元反射率(模拟端元), 最后用带约束条件的线性模型进行混合像元分解。用浙江省安吉县毛竹林调查资料及 Landsat TM 对该方法进行验证和对比分析表明, 基于模拟端元的混合像元分解结果比基于影像端元和参考端元的精度高且具有良好的稳健性。模拟真实场景的混合像元分解方法将样地调查数据的先验知识应用于端元提取, 并将三维模拟模型引入到二维的线性光谱分解中, 具有一定的优势和应用推广前景。

关键词: 场景建模, 模拟端元, 像元分解, 线性模型, Landsat TM

中图分类号: TP751　　**文献标志码:** A

引用格式: 范渭亮, 杜华强, 周国模, 徐小军, 崔瑞蕊, 董德进. 2010. 模拟真实场景的混合像元分解. 遥感学报, **14**(6): 1241—1258

Fan W L, Du H Q, Zhou G M, Xu X J, Cui R R and Dong D J. 2010. Spectral mixture analysis method based on the simulation of real scenario. *Journal of Remote Sensing*. **14**(6): 1241—1258

1 引　言

通常, 遥感影像是以像元为单位描述地物目标属性的一种信息载体。在像元尺度内通常有多种地物类型或同一地物类型的不同状态对遥感影像获取的信息产生影响, 这种现象称为"混合像元问题"。混合像元不仅影响识别地物目标的精度, 也是遥感科学定量化发展的主要障碍(杨伟等, 2008)。为了解决混合像元产生的一系列问题, 针对不同问题发展了相应的像元分解方法(Ichoku & Karnieli, 1996; Roberts 等, 1998)。赵英时(2003)总结了适用于不同场合的混合像元分解模型, 包括线性模型、几何光学模型、随机几何模型、概率模型和模糊模型。

端元的质量是影响像元分解结果重要的因素(赵英时,2003)。目前, 端元的选择主要有以下两种方法:

第 1 种为影像端元法通过不同的分析方法在遥感影像上确定端元的方法。确定这一类端元不需要进行实地的光谱测量, 也不需要额外的先验知识, 因此这一种端元选择方法是目前较普遍使用的方法(Woodcock 等, 1994, 1997; Scarth & Phinn, 2000; Franklin & Turner, 1992)。然而, 在像元分解过程中经常出现遥感影像中无法找到需要的"纯净像元"(Tompkins 等, 1997; 陶雪涛等, 2008)。比如, Li 和 Strahler(1985, 1986, 1992)提出的几何光学模型, 其中的四分量包括植被承照面, 植被阴影面, 背景承照面, 背景阴影面, 但四分量理想的纯净像元在遥感影像上不可能存在的。一般的解决方法是用洁净并且深的水体代替阴影分量(Hall 等, 1995)或在"穗帽变换"亮度和绿度两个分量的二维散点图中搜索近似的纯净像元(Li & Strahler,1985; Woodcock 等, 1994, 1997)。影像端元很难反映地物目标的真实属性。

第 2 种为参考端元法, 即将野外实测的波谱直接作为端元或从光谱库中选择端元 (Rashed 等, 2003)。参考端元从理论上讲可以比较精确的代表地物反射特征, 但遥感影像受大气、地形、传感器等

收稿日期: 2009-10-15; 修订日期: 2010-05-15

基金项目: 国家自然科学基金项目(编号: 30700638); 国家林业局 948 项目(编号:2008-4-49)和浙江省科技厅项目(编号: 2007C13041, 2008C12068)。

第一作者简介: 范渭亮(1984—), 男, 浙江农林大学硕士研究生, 目前主要从事林业遥感研究, 发表论文 1 篇。E-mail: fanweiliang@163.com。

通讯作者: 杜华强, E-mail: dhqrs@126.com。

诸多外界因素影响，因此参考端元往往很难代表遥感影像中地物的光谱反射特征。另外，参考端元一般只能代表某种确定地物类型的反射率，在像元分解过程中如果漏选了某种地物类型的端元，会造成很大的分解误差甚至错误。

植被的三维建模目前已在农学、林学、生态学、遥感等领域广泛应用(郭焱&李保国，2001)。在遥感应用中，Disney 等(2000)总结了可以用来生成场景的方法。随着计算机技术、图形学算法的快速发展，以及三维植物测量与建模的不断涌现(Prusinkiewicz, 1998)，适用于多种场合通用模型的研究正不断发展(梁顺林，2009)。更精确的模拟植被冠层细节有助于提高模型的精度，然而，目前对于林分尺度场景细节模拟的最大障碍是场景中面元数量过多导致的计算机运行速度过慢甚至无法运行(雷向东等，2006)。在很多研究中已经采用了简化模型的方法并取得了较好的效果(Morsdorf 等，2004; Li & Strahler, 1985, 1986)。

在真实的森林场景中，传感器接收到的光线主要来自于 4 个部分，即上文所说的四分量。考虑到实际需要和问题的简化，以及影像端元和参考端元的缺点，本文以毛竹林为例，在简化的植物模型基础上进行真实场景的模拟；从模拟场景中获取上述四分量面积比例，根据面积比例采用最小二乘法反演四个分量的反射率(本文称为模拟端元)；最后根据模拟端元，使用含有全部约束条件的线性模型进行混合像元分解，获得非建模像元四分量的丰度。为了评价基于模拟端元混合像元分解的精度，以毛竹林郁闭度为例，对影像端元、参考端元以及模拟端元的分解结果进行比较。

2 研究方法

2.1 样地数据获取与遥感影像预处理

研究区为浙江省安吉县，外业样地调查于 2008 年 8 月下旬到 9 月初完成。共调查 55 个 30m×30m 的毛竹纯林样地。通过每木检尺获得样地内毛竹的胸径和株数。在样地调查的同时对样地中心点进行 GPS 手持机单点定位。毛竹林郁闭度的调查为浙江农林大学林业专家及安吉县林业局的专业调查人员按照国家林业局 2003 年颁布的《森林资源规划设计调查主要技术规定》通过目测法获取，相对误差在 10%以内。2009-09-06 采用 ASD 光谱仪分别实测了毛竹及林内地面光照和阴影条件下的高光谱反射率，多次测量取平均值作为最终结果，光谱测量的季节与外业调查的季节一致，能够真实反映毛竹林四分量反射特征。

根据真实场景建模的需要，通过实测的毛竹胸径，采用周芳纯(1981)建立的模型计算得到单株毛竹全高、枝下高，根据相关文献(周芳纯，1982)计算毛竹的冠幅。将计算得到的冠幅与 2008-09-30 实测的毛竹冠幅进行比较，两者相关系数达到 0.88，完全可以满足本研究的需要。

卫星遥感数据为 2008-07-05 获取的 Landsat5-TM 数据。通过 1:50000 的地形图对影像进行几何精校正，总精度为 0.29 个像元。使用 ENVI4.4 中的 FLAASH 模块对遥感影像进行大气校正，将 DN 值转换为绝对反射率。

2.2 混合像元的线性分解

线性光谱混合理论认为，遥感影像中任一波段任一像元的光谱反射率是其各分量光谱响应的线性和。因此，像元第 i 波段的反射率 f_i 可以表示为

$$f_i = \sum_{j=1}^{n}(a_{ij}x_j) + e_i \tag{1}$$

式中，a_{ij} 是第 i 波段第 j 分量(j=1,2,⋯,n)的反射率，x_j 为第 j 分量在这一像元的面积中所占比例，e_i 是这一像元在第 i 波段的误差项。为了防止面积比例小于 0 或者大于 1 的情况，本文使用带全约束的最小二乘法求解各分量的面积比例。约束条件如式(2)和式(3)。

$$\sum_{j=1}^{n} x_j = 1 \tag{2}$$

$$x_j \geqslant 0 \tag{3}$$

2.3 影像端元

采用纯净像元指数(pixel purity index, PPI)方法在 TM 影像中查找光谱最纯净的像元(Boardman 等，1995)。在纯净像元指数的基础上，通过 N 维散点图结合原始遥感影像标定最终的端元，经过反复实验确定各分量的最优端元。

2.4 参考端元

采用便携式野外光谱测量仪(ASD)进行光谱测量。分别将测量的光照毛竹、阴影毛竹、毛竹林内光照地面以及毛竹林内阴影地面的反射光谱作为四分量端元的反射率。为了与 TM 影像的波段范围相匹配，将实测的高光谱反射率(图 1)根据 TM 的光谱响应函数重采样到 TM 的 6 个波段(TM1－5, TM 7)。

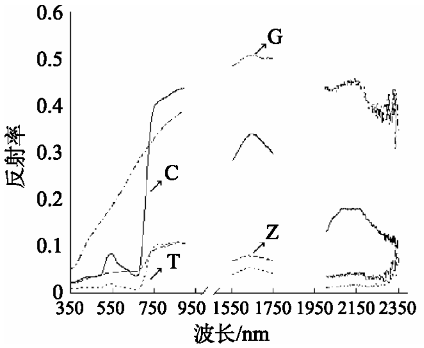

图 1　实测高光谱反射率

为了使参考端元在像元尺度上有效(李小文等, 1999), 根据以往的研究(李小文等, 1999; Raffy, 1994), 做以下假设: 像元内无地形起伏; 像元具有与亚像元相同的植被分布模式。

2.5　真实场景模拟及模拟端元的获取

在调查的55个样地中随机抽取了9个作为场景建模的样本。根据地面数据(包括样地的方位和坡度信息)和毛竹的冠型结构参数在 3DMax 9 中建立虚拟的三维场景模型, 为了解决像元尺度场景中面片数过多的问题, 本文将简化毛竹的几何形状, 同时, 将样地的背景地面假设为平面。结合遥感影像提供的太阳高度和方位信息模拟真实光照使目标地物产生阴影。统计观测天顶角为 0°时(同 TM 传感器)模拟样地四分量的面积比例。通过影像中对应像元的反射率和四分量的面积比例用最小二乘法求解端元各波段的反射率如式(4)。

$$\boldsymbol{A}_i=(\boldsymbol{X}^{\mathrm{T}}\cdot\boldsymbol{X})^{-1}\cdot\boldsymbol{X}^{\mathrm{T}}\cdot\boldsymbol{F}_i \tag{4}$$

式中, $\boldsymbol{A}_i$ 为第 i 波段的端元反射率向量, $\boldsymbol{F}_i$ 为 n 个像元第 i 波段的反射率向量, $\boldsymbol{X}$ 为 n 个像元的面积组分矩阵。由于本文将样地组分数定为 4, 因此必须满足 $n\geqslant 4$ 时, 式(4)才有恰定或超定方程的最小二乘解。

根据毛竹样地的实测数据, 将 9 个场景建模样本中每株毛竹根据其胸径计算得到的冠幅、枝下高、全高简化为“棒”加“胶囊体”的简单几何体, 见图 2。由于毛竹林单位面积株树过多, 一般 150—500 株/900m^2, 并且单株毛竹定位困难, 因此没有对每一株毛竹定位。为了解决毛竹在林内的位置问题, 在场景建模过程中随机产生毛竹在样地内的位置。根据上文描述建立的场景模型如图 3。其中, 对 2 号样地所有毛竹的位置随机赋值 10 次, 结果表明 10 次试验中四分量的面积比例变动范围在 2%—7%(图 4), 据此可以认为随机产生的位置对四分量所占像元面积比例的影响很小。

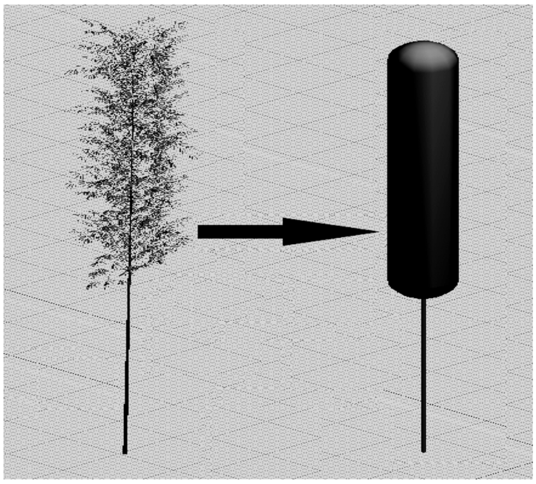

图 2 简化的毛竹模型

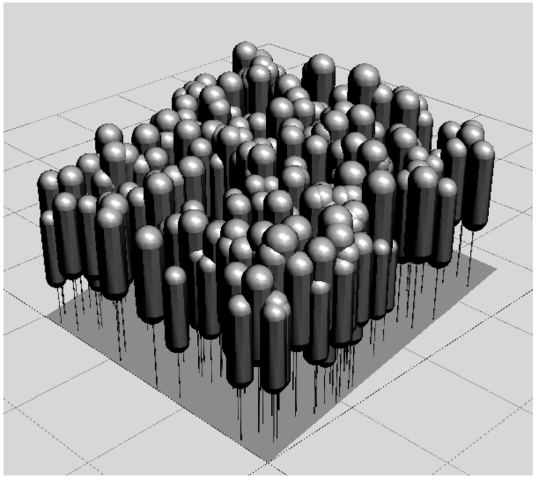

图 3　场景模拟模型

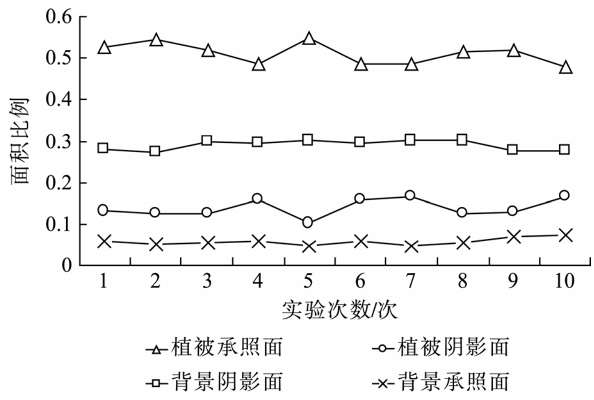

图 4　2 号样地毛竹位置随机赋值实验

根据对图 4 的分析, 对于 2 号样地可以选择任意一次实验进行像元分解。图 5 是 2 号样地第 5 次实验模拟场景的俯视图, 在图 5(a)中明显区分出毛竹林内的植被承照面、背景承照面和阴影这 3 个分量。图 5(b)是没有光源时样地像元的俯视图, 在图

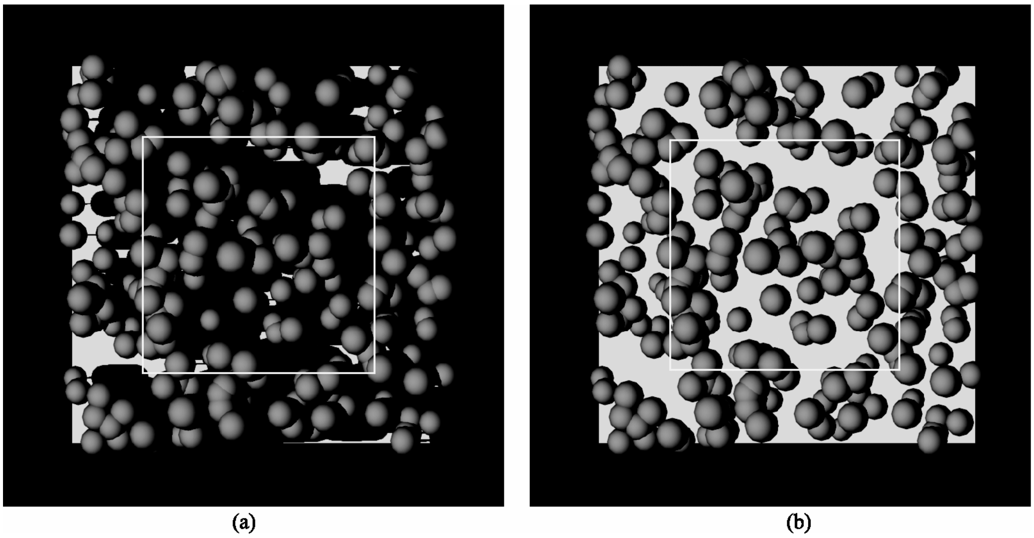

图 5　二号样地第 5 次实验模拟场景的俯视图
(a) 有光源的俯视场景; (b) 无光源的俯视场景

5(b)中容易找到植被与非植被的分界面。因此，通过图 5(a)与图 5(b)的分类与加减运算可以得到建模样本毛竹林四分量的面积比例。

毛竹林一般是成片连续的森林，因此，模拟样地的边缘问题很明显(图 5)，即光照方向一侧样地光照背景明显偏多，同时，许多树冠超出了样地的边界。为了消除边缘的影响，必须进行边缘校正改善模拟的效果。对于边缘校正问题，Li 和 Strahler(1985)已经进行了讨论。根据线性光谱混合理论和样地中心 50%正方形面积内的四分量比例基本不受边缘影响，只计算样地中心 50%正方形面积内的四分量比例作为整个像元的四分量面积比例(图 5)。

对所选的 9 个样地分别建立场景模型，通过场景模拟的方法确定每个样地内四分量的面积比例。通过式(4)计算出各波段四分量端元的反射率(图 6(c)。

2.6　精度评价方法

垂直视情况下，郁闭度等于四分量像元分解结果中植被承照面与植被阴影面的丰度之和(Woodcock 等, 1997)。本文采用实测的郁闭度对像元分解

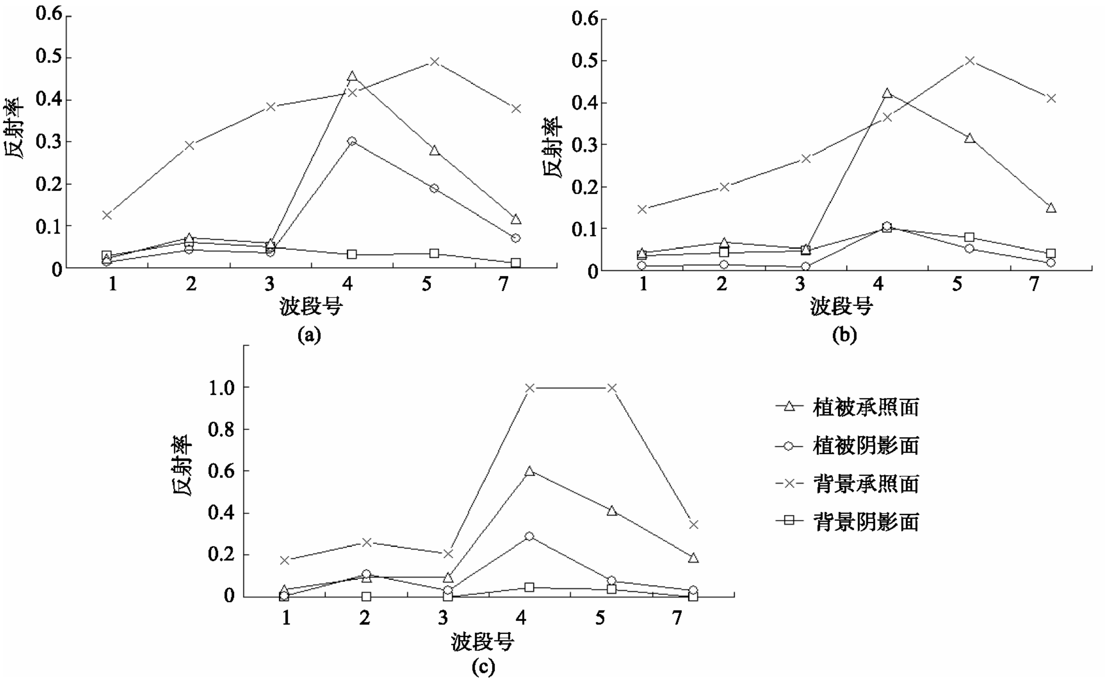

图 6　3 种端元获取的四分量反射率
(a) 影像端元; (b) 参考端元; (c) 模拟端元

的结果进行精度验证, 同时也对比将 3 种端元应用于真实遥感影像的像元分解结果。

3 结果与分析

3.1 场景模拟郁闭度与实测郁闭度的关系

从图 7 看出, 9 个模拟场景计算出的郁闭度与实测值有良好的线性关系。在中等郁闭度的情况下(0.5—0.8), 模拟效果较好; 在郁闭度大于 0.8 时, 郁闭度模拟值略低于实测值。这是由于随着郁闭度的增加, 随机设置坐标使树冠间部分甚至全部重叠造成的(Chen & Leblanc,1997)。

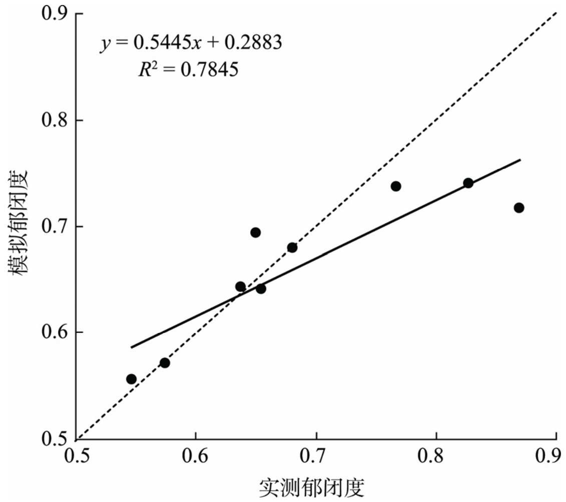

图 7 9 个建模样本的模拟郁闭度与其实测郁闭度的关系

3.2 三种端元的反射率

参考端元与影像端元差异相对较小, 说明未经尺度转换的地面光谱数据在像元尺度可以得到较好的表达(图 6)。参考端元植被阴影面的反射率在各波段都较低, 这是因为在测量时阴影过多的遮住了入射光线, 使参考端元各波段(尤其是 TM4)反射率急剧下降所致。

模拟端元与另外两种端元的反射率总体差别较大。模拟端元植被承照面的反射率理论上模拟了100%郁闭度情况下光照植被的反射率, 随着叶片数量的增加, TM 各波段的反射率会增加(徐希孺,2005), 因此模拟端元植被承照面的反射率整体较高; 模拟端元与影像端元植被阴影面的光谱特征相似, 较好的反映了植被的特点; 与影像端元和参考端元的背景承照面表现出土壤特征不同, 模拟端元的背景承照面表现出植被特征, 同时, 模拟端元的背景阴影面也表现出了植被特征, 这是因为模拟端元背景面的反射光谱包含了林下植被、枯落物等众多因子的综合信息。

3.3 像元分解精度验证

用 55 个样地实测的郁闭度验证像元分解的结果。从图 8 看出, 影像端元和参考端元郁闭度真实值与实测值之间线性关系较差, 同时, 郁闭度高估的现象严重, 相对误差多数在 40%左右(图 9)。根据对图 6 三种端元反射率的比较, 影像端元和参考端元方法的结果高估了郁闭度主要是因为这两种方法低估了对于植被承照面的端元反射率。模拟端元像元分解得到的预测值与实测值之间线性相关性相对较好, 并且极显著(图 8(c))。一般认为, 郁闭度的估计误差在10%以内是可以接受的(Liu & Wu, 2005), 图 9 表明, 只有少数样地误差超出了这个范围。

3.4 实际遥感数据实验

为了进一步对比像元分解的效果, 在安吉县境内选择一片相对连续毛竹林区域的遥感影像(196 行, 172 列)进行混合像元的线性分解。这一区域包含了少量的道路和城镇, 不包括真实场景模拟使用的 9 个样地中任何一个。

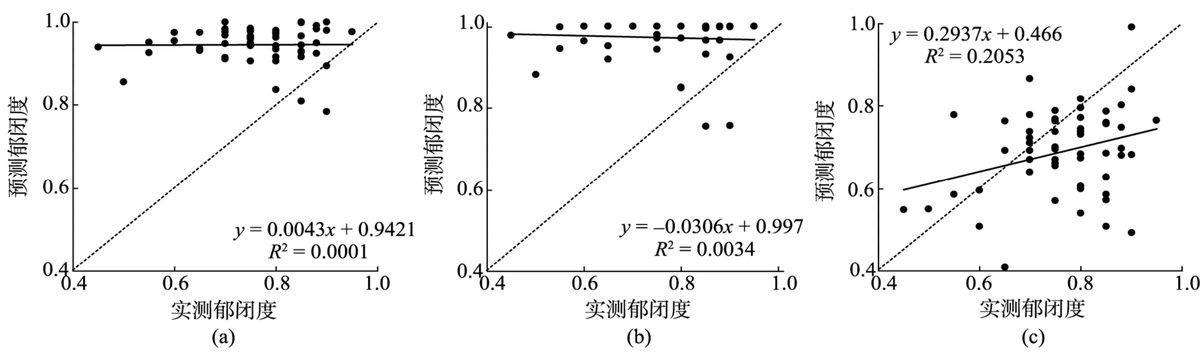

图 8 55 个样地的预测郁闭度与其实测郁闭度的关系

(a) 影像端元; (b) 参考端元; (c) 模拟端元

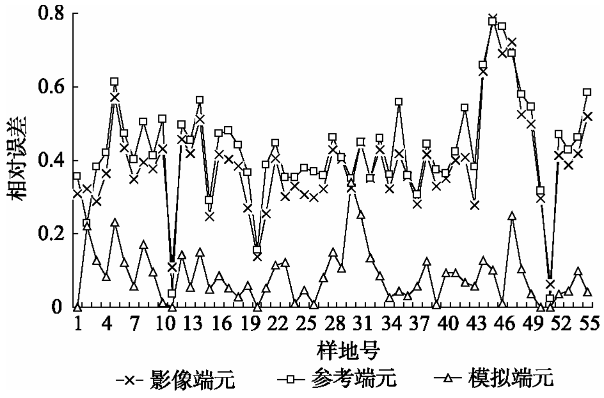

图 9 3 种不同端元预测郁闭度与实测郁闭度的相对误差

图 10 是 3 种端元对实验影像进行像元分解的结果。基于影像端元的分解结果中毛竹林区域两个背景分量的丰度接近 0，而两个植被分量则夸张了在阴阳坡植被覆盖度的差别，与实地的观察明显不符。参考端元中植被承照面的丰度接近 100%，而另外 3 个分量的丰度接近 0，明显夸张了植被承照面的丰度而低估了另外 3 个分量。相对而言，模拟端元各种组分的丰度合理，且在影像中分布均匀，符合毛竹林同质、均匀的特性(张刚华等，2007)，像元分解后目视效果较好。

统计实验影像不同方法像元分解后的郁闭度并绘制直方图(图 11)，从数值上进一步说明遥感影像像元分解的结果。与实测郁闭度相比，影像端元方法整体高估了实验影像的郁闭度，而参考端元方法的郁闭度分布与实测郁闭度分布差异巨大。模拟端元像元分解得到的郁闭度分布状况则与实测郁闭度分布曲线接近，进一步说明模拟端元具有一定的优势，郁闭度估算精度较高。

4 讨 论

4.1 真实场景模拟及精度

分形方法或计算机图形学方法在植物三维建模过程中应用广泛，并且取得很好的效果(Garcia & Sommer, 2006; Disney 等, 2006)。然而，如何优化场

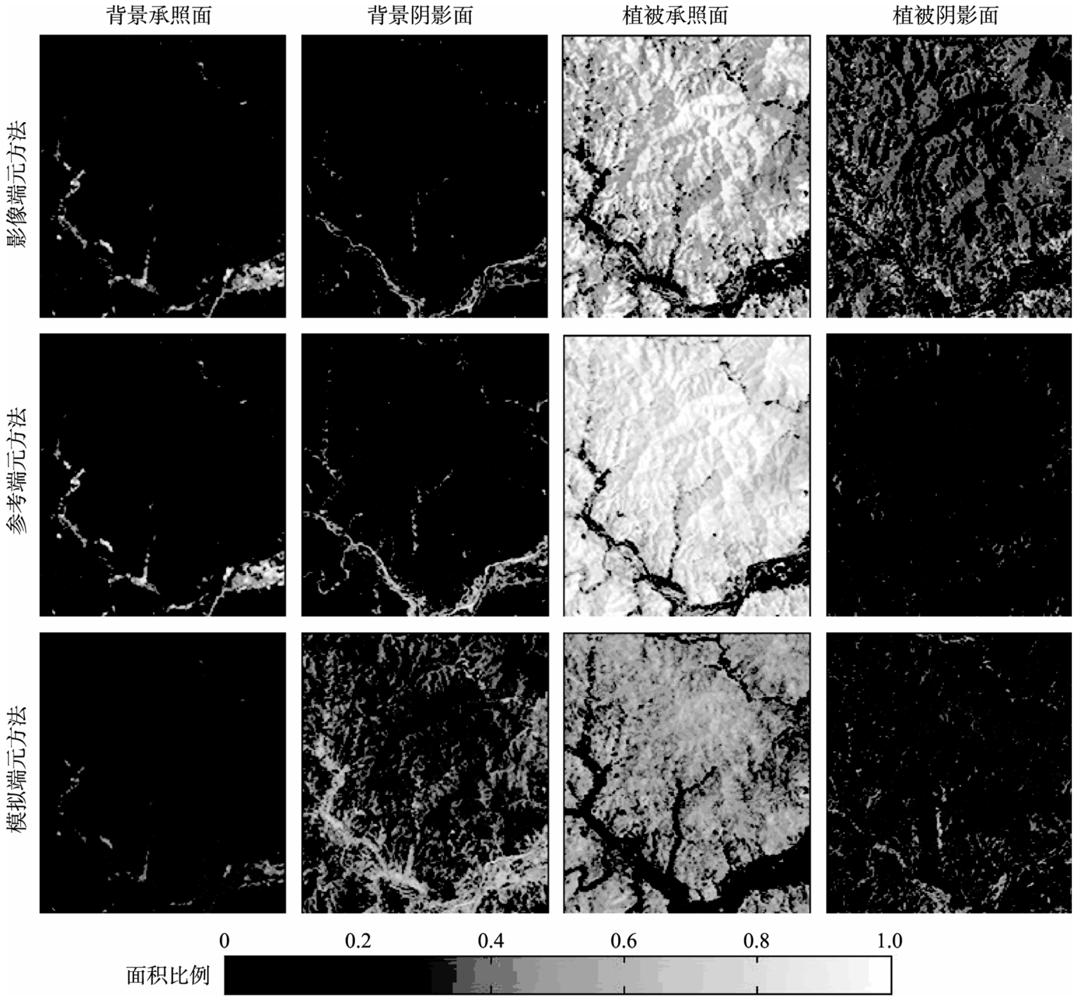

图 10 基于 3 种端元遥感数据像元分解结果

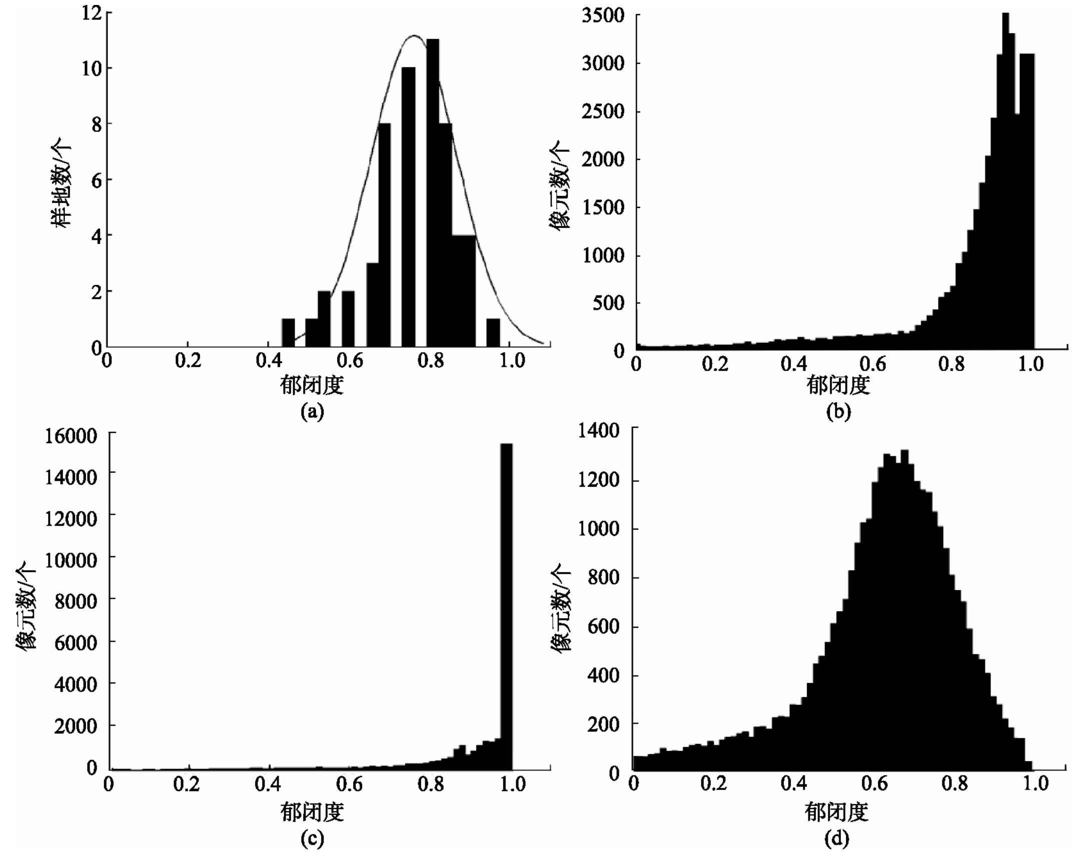

图 11 55 个毛竹样地郁闭度分布及基于 3 种端元遥感影像分解得到的毛竹林郁闭度分布对比

(a) 实测郁闭度分布; (b) 影像端元法郁闭度分布; (c) 参考端元法郁闭度分布; (d) 模拟端元法郁闭度分布

景中的面片数量却是林分尺度场景建模急需解决的问题。在实际应用中，例如本文中的混合像元分解问题，可以根据需要和目标尽量简化模型，这样不仅节省大量的时间和空间，还有利于解释问题的机理与本质。本文采用简化的植物模型进行真实场景的模拟并取得了较好的效果。

尽管真实场景的模拟取得了较好的效果，但仍然存在一些值得探讨的问题。首先，模拟真实场景需要大量的地面及冠型实测数据作为先验知识，如何从这些先验知识中筛选有用信息并将其作为模型简化的依据是一个值得研究的问题。其次，场景模拟过程的误差来源及误差分析也是一个值得探讨的问题，根据对场景郁闭度模拟值与实测值的分析(图7)，虽然模拟端元相对于其他两种端元精度最高，但相关指数较低(R^2=0.205)，其中有几个样地的误差在 3 种端元都比较大，如果去掉这些样地会得到较高的精度，但这是随机误差还是固有特征有待进一步分析。同时，由于无法模拟实际样地中的起伏以及由此形成的阴影，本文将样地的背景假设为平面。虽然在样地范围内(30m×30m)地形的变化很小，但这也可能是模拟端元的部分误差来源。最后，场景建模样本数量的选择也是今后研究的一个重要内容，本文仅在 55 个样地中随机挑选了 9 个作为场景建模的样本，究竟选择多少个样本进行建模可以获得最佳的效果需要进一步讨论。

将模拟真实场景的混合像元分解方法应用于毛竹林四分量的像元分解，对于其他类型的地物目标，如果能获得相应的地面调查数据，也可以根据本文的思路进行推广应用。

4.2 端元光谱反射率及线性混合像元分解

如前所述，影像端元较难反映地物目标的真实属性，对参考端元进行了假设后用于像元尺度，尽管实测光谱数据与像元尺度的影像端元相似并得到了相同的结论，但这种做法仍有可能造成一定的不确定性(李双成 & 蔡运龙, 2005)，有待于进一步研究。模拟端元具有良好的特性，首先，在没有选择林下背景作为端元的情况下，模拟端元较好的反映了包含在像元反射率中的林下背景信息，这克服了难以获取林下信息和端元选择不完全的缺点，从而使本文提出的模型具有良好的稳健性。其次，模拟端元的植被承照面反射率高于其他两种端元的反射率

(图 6)，在一定程度上反映模拟端元中毛竹林反射率受其他因素影响较小，说明模拟端元在理论上得到了较为“纯净”植被承照面反射率，即克服了影像端元“不纯”的缺点。当然模拟端元通过四分量反演得到，在像元尺度上背景面可以反映林下信息，代表的可能是混合地物类型的反射率，然而这并不影响对像元分解结果的理解。

混合像元分解模型包括 5 种主要的模型，本文仅采用线性模型进行混合像元分解，其他混合像元分解方法是否会得到相同的结果需要进一步对比分析。

本文没有选用安吉县整景遥感影像作为实际遥感数据实验主要是考虑了以下几点。第一，研究区域内地物类型复杂，对整景影像进行混合像元分解不利于目视判读；第二，本文中像元分解使用全约束最小二乘法，求解时多次用到矩阵的乘积及求逆，所需的时间复杂度大(童庆禧，2006)；第三，选用实验区域的影像不包含任何场景建模样本，像元分解结果更能体现真实场景模型的稳健性。因此，将模拟端元应用于较大区域混合像元分解还有一些技术问题特别是地物类型的复杂性和数学算法等方面需要深入研究。

5 结 论

总结了混合像元分解的方法，提出了原有方法中存在的问题。为了克服原有像元分解方法中端元选择的局限性，以毛竹林四分量的像元分解为例，采用模拟真实场景获取端元的方法进行混合像元分解，然后与影像端元和参考端元的混合像元分解结果对比，研究表明模拟端元的混合像元分解结果精度最高，同时具有良好的稳健性。随后，又选择了遥感影像中的一块区域进行混合像元分解，同样取得了最好的效果。模拟真实场景的混合像元分解方法采用样地调查数据作为先验知识应用于端元提取，同时将三维模拟模型引入到二维的线性光谱分解当中使得模拟端元更能反映真实情况，具有一定的优势和应用前景。

REFERENCES

Boardman J W, Kruse F A and Green R O. 1995. Mapping target signatures via partial unmixing of AVIRIS data: in Summaries. Fifth JPL Airbone Earth Science Workshop. JPL Publication, **1**: 23—26

Chen J M and Leblanc S G. 1997. A four-scale bi-directional reflectance model based on canopy architecture.*IEEE Transactions on Geoscience and Remote Sensing*, **35**: 1316—1337

Disney M I and Lewis S P. 2006. 3D modeling of forest canopy structure for remote sensing simulations in the optical and microwave domains. *Remote Sensing of Environment*, **100**: 114—132

Disney M I, Lewis S P and North P R J. 2000. Monte carlo ray tracing in optical canopy reflectance modeling. *Remote Sensing Reviews*, **18**(2—4): 163—196

Franklin J and Turner D L. 1992. The application of a geometric optical canopy reflectance model to semiarid shrub vegetation. *IEEE Transactions on Geoscience and Remote Sensing*, **30**(2): 293—301

Garcia-Haro F J and Sommer S. 2002. A fast canopy reflectance model to simulate realistic remote sensing scenarios. *Remote Sensing of Environment*, **81**: 205—227

Guo Y and Li B G. 2001. Research of review virtual plant.*Chinese Science Bulletin*, **46**(4): 273—280

Hall F G, Shimabukuro Y E and Huemmrich K F. 1995. Remote sensing of forest biophysical structure using mixture decomposition and geometric reflectance models. *Ecology Applications*, **5**(4): 993—1013

Ichoku C and Karnieli A. 1996. A review of mixture modeling techniques for sub-pixel land cover estimation. *Remote Sensing Reviews*, **13**: 161—186

Lei X D, Chang M, Lu Y C and Zhao T Z. 2006. A review on growth modeling and visualization for virtual trees. *Scientia Silvae Sinicae*, **42**(11): 123—131

Li S C and Cai Y L. 2005. Some scaling issues of geography. *Geographical research*, **24**(1): 11—18

Li X W and Strahler A H. 1985. Geometric-optical modeling of a conifer forest canopy. *IEEE Transactions on Geoscience and Remote Sensing*, **23**: 705—721

Li X W and Strahler A H. 1986. Geometrical-optical reflectance modeling of a conifer forest canopy. *IEEE Transactions on Geoscience and Remote Sensing*, **24**: 906—919

Li X W and Strahler A H. 1992. Geometric-optical bidirectional reflectance modeling of the discrete crown vegetation canopy: Effect of crown shape and mutual shadowing. *IEEE Transactions on Geoscience and Remote Sensing*, **30**: 276—291

Li X W, Wang J D and Strahler A H. 1999. Scale effects of planck law over a non-isothermal blackbody surface. *Science in China (Series E)*, **29**(5): 422—426

Liang S L. 2009. Quantitative Remote Sensing. (Fan W J Trans). Beijing: Science Press

Liu W and Wu E Y. 2005. Comparison of non-linear mixture models: sub-pixel classification. *Remote Sensing of Environment*, **94**: 145—154

Morsdorf F, Meier E, Kötz B, Itten K I, Dobbertin M and Allgöwer B. 2004. LIDAR-based geometric reconstruction of boreal type forest stands at single tree level for forest and wildland fire management. *Remote Sensing of Environment*, **92**(3): 353—362

Przemyslaw Prusinkiewicz. 1998. Modeling of spatial structure and development of plants: a review. *Scientia Horticulture*, **74**(1—2): 113—149

Raffy M. 1994. Heterogeneity and change of scale in models of remote sensing, Spatialization of multi-spectral models. *International journal of remote sensing*, **15**(12): 2359—2380

Rashed T, Weeks J R, Roberts D, Rogan J and Powell R. 2003. Measuring the physical composition of urban morphology using multiple endmember spectral mixture models. *Photogrammetric Engineering & Remote Sensing*, **69** (9): 1011—1020

Roberts D A, Batista G T, Pereira J L G, Waller E K and Nelson B W. 1998. Change identification using multi-temporal spectral mixture analysis. Applications in Eastern Amazonia. Remote Sensing Change Detection: Environmental Monitoring Applications and Methods. Michigan: Ann Arbor Press

Scarth P and Phinn S. 2000. Determining forest structural attributes using an inverted geometric-optical model in mixed Eucalypt forest, Southeast Queensland, Australia. *Remote Sensing of Environment*, **71**: 141—157

Tao X T, Wang B and Zhang L M. 2008. New scheme for decomposition of mixed pixels of remote sensing images based on nonnegative matrix factorization. *Information and Electronic Engineering*, **6**(1): 34—39

Tompkins S, Mustard J F, Pieters C M and Forsyth D W. 1997. Optimization of endmembers for spectral mixture analysis.*Remote Sensing of Environment*, **59**: 472—489

Tong Q X, Zhang B and Zheng L F. 2006. Hyperspectral Remote Sensing - Principles, Technology and Application. Beijing: Science Press

Woodcock C E, Collins J B, Gopal S, Jakabhazy V D, Li X W, Macomber S A, Ryherd S, Harward V J, Levitan J, Wu Y C and Warbington R. 1994. Mapping forest vegetation using Landsat TM imagery and a canopy reflectance model. *Remote Sensing of Environment*, **50**: 240—254

Woodcock C E, Collins J B, Jakabhazy V D, Li X W, Macomber S A and Wu Y C. 1997. Inversion of the Li-Strahler canopy reflectance model for mapping forest structure. *IEEE Transactions on Geoscience and Remote Sensing*, **35**(2): 405—414

Xu X R. 2005. Remote Sensing Physics.Beijing: Science Press

Yang W, Chen J, Song X W J, Gong P and Chen C X.2008.A new spectral mixture analysis method based on spectral correlation matching. *Journal of Remote Sensing*, **12**(3): 454—461

Zhang G H, Nie J Z and Xiao J H. 2007. Geostatistics analysis on the spatial pattern of Moso Bamboo.*Chinese Agricultural Science Bulletin*, **23**(12): 136—141

Zhao Y S. 2003. Principles and Methods of Analysis of Remote Sensing Applications. Beijing: Science Press

Zhou F C. 1981. Studys on the structure of culm form of phyllostachys pubescens. *Journal of Nanjing Technological College of Forest Products*, **1**: 16—69

Zhou F C. 1982. Studys on the structure of bamboo crown of phyllostachys pubescens. *Journal of Nanjing Technological College of Forest Products*, **3**: 46—73

附中文参考文献

郭焱，李保国．2001．虚拟植物的研究进展．科学通报，**46**(4): 273—280

雷向东，常敏，陆元昌，赵天忠．2006．虚拟树木生长建模及可视化研究综述．林业科学, **42**(11): 123—131

梁顺林. 2009.定量遥感．范闻捷译．北京：科学出版社

李双成，蔡运龙．2005．地理尺度转换若干问题的初步探讨．地理研究, **24**(1): 11—18

李小文，王锦地，Strahler A H. 1999．非同温黑体表面上 Planck 定律的尺度效应．中国科学(E 辑), **29**(5): 422—426

陶雪涛，王斌，张立明. 2008．基于 NMF 的遥感图像混合像元分解新方法．信息与电子工程, **6**(1): 34—39

童庆禧，张兵，郑兰芬. 2006．高光谱遥感-原理、技术与应用．北京：高等教育出版社

徐希孺. 2005．遥感物理．北京：科学出版社

杨伟，陈晋，松下文经，宫鹏，陈春晓. 2008．基于相关系数匹配的混合像元分解算法．遥感学报, **12**(3): 454—461

张刚华，聂洁珠，萧江华．2007．毛竹种群空间格局的地统计学分析．中国农学通报, **23**(12): 136—141

赵英时. 2003．遥感应用分析原理与方法.北京:科学出版社

周芳纯. 1981．毛竹秆形结构的研究．南京林产工业学院学报, **1**: 16—69

周芳纯．1982．毛竹林冠结构研究．南京林产工业学院学报，**3**: 46—73